Published in final edited form as:
Hepatology. 2015 March ; 61(3): 915–929. doi:10.1002/hep.27339.

Astrocyte elevated gene-1 (AEG-1) and c-Myc cooperate to promote hepatocarcinogenesis

Jyoti Srivastava[1], **Ayesha Siddiq**[1], **Rachel Gredler**[1], **Xue-Ning Shen**[1], **Devaraja Rajasekaran**[1], **Chadia L. Robertson**[1], **Mark A. Subler**[1], **Jolene J. Windle**[1], **Catherine I. Dumur**[2], **Nitai D. Mukhopadhyay**[3], **Dawn Garcia**[4], **Zhao Lai**[4], **Yidong Chen**[5], **Uthra Balaji**[6], **Paul B. Fisher**[1,7,8], and **Devanand Sarkar**[1,7,8,9]

[1]Department of Human and Molecular Genetics, Virginia Commonwealth University, Richmond, VA 23298, USA

[2]Department of Pathology, Virginia Commonwealth University, Richmond, VA 23298, USA

[3]Department of Biostatistics, Virginia Commonwealth University, Richmond, VA 23298, USA

[4]Greehey Children's Cancer Research Institute, University of Texas Health Science Center San Antonio, San Antonio, TX 78229

[5]Computational Biology and Bioinformatics, University of Texas Health Science Center San Antonio, San Antonio, TX 78229

[6]Department of Pathology, Simmons Cancer Center, UT Southwestern Medical Center, Dallas, TX

[7]VCU Massey Cancer Center, Virginia Commonwealth University, Richmond, VA 23298, USA

[8]VCU Institute of Molecular Medicine (VIMM), Virginia Commonwealth University, Richmond, VA 23298, USA

Abstract

Astrocyte elevated gene-1 (AEG-1) and c-Myc are overexpressed in human hepatocellular carcinoma (HCC) functioning as oncogenes. AEG-1 is transcriptionally regulated by c-Myc and AEG-1 itself induces c-Myc by activating Wnt/β-catenin signaling pathway. We now document cooperation of AEG-1 and c-Myc in promoting hepatocarcinogenesis by analyzing hepatocyte-specific transgenic mice expressing either AEG-1 (Alb/AEG-1), c-Myc (Alb/c-Myc) or both (Alb/AEG-1/c-Myc). WT and Alb/AEG-1 mice did not develop spontaneous HCC. Alb/c-Myc mice developed spontaneous HCC without distant metastasis while Alb/AEG-1/c-Myc mice developed highly aggressive HCC with frank metastasis to the lungs. Induction of carcinogenesis by N-nitrosodiethylamine (DEN) significantly accelerated the kinetics of tumor formation in all groups. However, in Alb/AEG-1/c-Myc the effect was markedly pronounced with lung metastasis. *In vitro* analysis showed that Alb/AEG-1/c-Myc hepatocytes acquired increased proliferation and transformative potential with sustained activation of pro-survival and epithelialmesenchymal

[9]**Corresponding author:** 1220 East Broad St, PO Box 980035 Richmond, VA 23298 Tel: 804-827-2339 Fax: 804-628-1176 dsarkar@vcu.edu.

The authors declare no conflict of interest.

transition (EMT) signaling pathways. RNA-sequencing analysis identified a unique gene signature in livers of Alb/AEG-1/c-Myc mice that was not observed when either AEG-1 or c-Myc was overexpressed. Specifically Alb/AEG-1/c-Myc mice overexpressed maternally imprinted non-coding RNAs, such as Rian, Meg-3 and Migr, which are implicated in hepatocarcinogenesis. Knocking down these ncRNAs significantly inhibited proliferation and invasion by Alb/AEG-1/c-Myc hepatocytes.

Conclusion—Our studies reveal a novel cooperative oncogenic effect of AEG-1 and c-Myc that might explain the mechanism of aggressive HCC. Alb/AEG-1/c-Myc mice provide a useful model to understand the molecular mechanism of cooperation between these two oncogenes and other molecules involved in hepatocarcinogenesis. This model might also be of use for evaluating novel therapeutic strategies targeting HCC.

Keywords

AEG-1; c-Myc; hepatocarcinogenesis; metastasis; ncRNA

Introduction

Astrocyte elevated gene-1 (AEG-1), also known as Metadherin (MTDH) or LYRIC, is overexpressed in all cancers studied to date (1). In hepatocellular carcinoma (HCC), a high percentage of patients demonstrate AEG-1 overexpression in both mRNA and protein levels (2, 3). In HCC patients, AEG-1 expression is closely associated with microvascular invasion, pathologic satellites, tumor differentiation, and TNM stage and both overall survival and cumulative recurrence rates show an inverse correlation with AEG-1 expression levels (3, 4). ‘Gain-of-function’ and ‘loss-of-function’ studies using human HCC cell lines confirmed that AEG-1 confers highly aggressive, angiogenic, metastatic and chemoresistance phenotypes (2, 5-7). A transgenic mouse with hepatocyte-specific overexpression of AEG-1 (Alb/AEG-1) did not develop spontaneous HCC, however, upon treatment with the chemical carcinogen N-nitrosodiethylamine (DEN) HCC developed with a significantly accelerated kinetics with increased angiogenesis and chemoresistance (8). Collectively, these studies indicate that although AEG-1 itself may not initiate HCC it plays a key role in HCC progression and metastasis.

Multiple mechanisms underlie AEG-1 overexpression in cancer that include amplification of the *AEG-1* locus 8q22, regulation by multiple tumor suppressor miRNAs and post-translational regulation by monoubiquitination that increases stability of AEG-1 protein (2, 9-14). The oncogenic transcription factor c-Myc directly binds to the AEG-1 promoter and regulates its transcription (15). Overexpression of c-Myc is detected in a high percentage of HCC patients (16, 17) and thus might be a key mechanism by which AEG-1 expression is induced in HCC. Gain of chromosome 8q is a defining feature of human HCC leading to co-amplification of AEG-1 and c-Myc, the latter located at 8q24.1 (18). On the other hand, AEG-1 itself induces c-Myc expression by activating the Wnt/β-catenin signaling pathway (2). AEG-1 also interacts with PLZF, a transcriptional repressor, inhibiting its ability to interact with the c-Myc promoter thereby inducing c-Myc expression (19). Thus AEG-1 and c-Myc provide a feedback loop promoting tumorigenesis.

c-Myc overexpression is a very common event in HCC. Genomic amplification of 8q24.1, the locus of the *c-Myc* gene is a frequent event in human HCC patients and c-Myc expression levels correlate with poor prognosis (17). Overexpression of c-Myc in mouse models induces HCC while antisense inhibition of c-Myc reverses this process (20-24). Using a Tet-Off system it was documented that overexpression of c-Myc induced HCC and turning c-Myc expression off by doxycycline treatment in the tumors resulted in marked tumor reduction with induction of differentiation (25). Removal of doxycycline, hence c-Myc reactivation, immediately restored neoplastic transformation. Collectively, these studies indicate that c-Myc is sufficient to induce HCC and is required to maintain the neoplastic state.

The present studies concentrated on defining how AEG-1 and c-Myc cooperate in promoting hepatocarcinogenesis since both are overexpressed in HCC. We show that hepatocyte-specific AEG-1 and c-Myc transgenic mice (Alb/AEG-1/c-Myc) develop highly aggressive, metastatic HCC, either spontaneously or DEN-induced, when compared to transgenic mice expressing either oncogene alone. RNA sequencing analysis demonstrated a distinct gene signature in the double transgenic mice that might confer this aggressive phenotype. These findings shed light into new mechanisms by which oncogenes cooperate in development and progression of HCC.

Experimental procedures

Mouse models

Alb/AEG-1 and Alb/c-Myc mice, generated in B6/CBA background, were described previously (8, 24). Alb/c-Myc was a kind gift from Dr. Snorri Thorgeirsson (NIH/NCI). Heterozygote Alb/AEG-1 and Alb/c-Myc mice were crossed to obtain WT, single transgenic and double transgenic littermates. Only male mice were used for experiments. For chemical carcinogenesis, mice were given a single i.p. injection of DEN (10 μg/gm) at 2 weeks of age. VCU IACUC approved the experiments and the animals were treated in ethical and humane ways.

Cell culture

Primary mouse hepatocytes were isolated from adult mice (3-5 months old) as described (8) and were cultured in Williams E medium containing $NaHCO_3$, L-glutamine, insulin (1.5 μM) and dexamethasone (0.1 μM) at 37°C and in 5% CO_2. Insulin was not added when the cells were cultured in basal media. Cell proliferation was analyzed by MTT and BrdU incorporation assays (2, 8). Senescence was detected by γ-H2AX foci and senescence-associated β-galactosidase assays (8). Invasion was analyzed by Matrigel invasion assays (2). Transformation was analyzed by focus formation assays in which primary hepatocytes were plated in confluence and allowed to form foci by overcoming contact-inhibition. 804G rat bladder carcinoma cells, a kind gift from Dr. Douglas E. Brash (Yale University School of Medicine), were cultured in MEM medium containing 2 mM L-glutamine, 20% FBS, 100 U/mL penicillin, and 100 μg/mL streptomycin at 37°C and in 5% CO_2. Cell-free extracellular matrix (ECM) was prepared by removing cytoplasm and nuclei from the deposited ECM as described (26). Briefly, 804G cells were plated at 50-70% confluence and

allowed to deposit ECM for 48 hr. The cells were washed with PBS and fresh 20 mM NH_4OH was added until cells were completely lysed as assessed microscopically. Remaining ECM was washed three times with PBS. For colony formation assay 2.5×10^5 mouse hepatocytes were plated on 804G ECM plates and cultured for 3 weeks. Colonies were counted using ImageJ software and colonies with more than 20 pixels were enumerated.

RNA sequencing (RNA-Seq)

Total RNA, extracted using Qiagen miRNAeasy mini kit (Qiagen, Valencia, CA) from livers of 3 adult mice per group, was employed for RNA sequencing. RNASeq library was prepared using Illumina TruSeq RNA sample preparation kit and sequenced on Illumina HiSeq2000 platform. RNA-Seq libraries were pooled together to aim about 25-40M read passed filtered reads per sample. All sequencing reads were aligned with their reference genome (UCSC mouse genome build mm9) using TopHat2 and the Bam files from alignment were processed using HTSeq-count to obtain the counts per gene in all samples. The counts were read into R software using DESeq package (27) and plot distributions were analyzed using Reads Per Kilobase Million (RPKM) values. Data were filtered based on low count or low RPKM value (<40 percentile). Pairwise tests were performed between each group using the functions in DESeq. Genes showing absolute fold-change of >2, FDR of <0.1 and p-value of <0.01 were selected.

RT-PCR

Total RNA was used for cDNA synthesis using High Capacity cDNA Reverse Transcription kit (Applied Biosystems). The primers used were: Rian: sense: 5′ CTAAGTCACCATGGAGAACCAG 3′, antisense: 5′ CAGATTTCAGGGTGGCAGTAAG 3′; Mirg: sense: 5′ CCACCATCATCAGAGAGCTTC 3′, antisense: 5′ GATGTAGCCTCTGGAGTCCTT 3′; Meg3: sense: 5′CCACCATCATCAGAGAGCTTC 3′, antisense: 5′ GAGCGAGAGCCGTTCGATG 3′; Tubb5: sense: 5′ GATCGGTGCTAAGTTCTGGGA 3′, antisense: 5′ AGGGACATACTTGCCACCTGT 3′.

Statistical analysis

Data were represented as the mean ± Standard Error of Mean (S.E.M) and analyzed for statistical significance using one-way analysis of variance (ANOVA) followed by Newman-Keuls test as a post hoc test. Additional Bayesian analysis is provided in supplement.

Results

We checked whether overexpression of AEG-1 and c-Myc might induce spontaneous hepatocarcinogenesis and metastasis. Alb/AEG-1 mice do not develop spontaneous tumors (8) while Alb/c-Myc mice develop HCC at ~10 months of age (22). However, distant metastases are not detected in Alb/c-Myc mice. We sacrificed one cohort of mice at 12 months of age with the presumption that at this age Alb/AEG-1/c-Myc mice might develop aggressive HCC with distant metastases. At this age WT and Alb/AEG-1 mice did not develop any tumors except for isolated nodules that are less than 2-mm in size (Table 1 and Fig. 1A). Alb/c-Myc mice presented with multiple small nodules that are less than 5-mm in

size. However, Alb/AEG-1/c-Myc mice developed tumors that are predominantly more than 5-mm in size (Table 1). At this time point metastases to lungs were not detected. We analyzed a second cohort of mice at 18 months of age. At this time point WT and Alb/AEG-1 mice developed few nodules less than 5-mm in size (Table 1 and Fig. 1A). Alb/c-Myc mice developed large tumors predominantly 10-20-mm in size. However, Alb/AEG-1/c-Myc mice presented with more aggressive phenotype with very large tumors, 10-20-mm or more than 20-mm in size, and in three mice the whole liver was converted into HCC with convergence of all nodules (Table 1). Most strikingly, all Alb/AEG-1/c-Myc mice developed lung metastases, which were not detected in any other groups of animals (Table 1).

We performed Bayesian statistical analysis to check the probability of tumorigenesis upon overexpression of AEG-1 and c-Myc using the following response variables: number and size of the nodules and the status of metastasis (Fig. 1B). The detailed methodology of analysis is presented in the supplement. The probability of no tumor formation was profoundly low in Alb/c-Myc and Alb/AEG-1/c-Myc mice (Fig. 1B). However the probability of the number of tumors was significantly higher in Alb/AEG-1/c-Myc mice when compared to other groups (Fig. 1B). Further analysis of probabilities based on tumor sizes also showed increased probability of larger tumors in Alb/AEG-1/c-Myc mice when compared to other groups (Fig. S1 & S2).

Histologically WT mice maintained normal liver architecture, Alb/AEG-1 mice presented with steatosis, as described previously (8), Alb/c-Myc mice showed features of hyperproliferative HCC (22) while Alb/AEG-1/c-Myc mice developed HCC over a steatotic background (Fig. 1C). Liver and tumor sections at 18 m of age were stained for AEG-1, c-Myc, HCC marker α-fetoprotein (AFP) and the proliferative marker PCNA (Fig. 1D). In WT liver low level AEG-1 was detected which was predominantly nuclear (8). Alb/AEG-1 livers showed increased AEG-1 expression both in the cytoplasm and nucleus which is consistent with the finding that overexpressed AEG-1 tends to accumulate in the cytoplasm (8). Interestingly, AEG-1 overexpression was detected also in Alb/c-Myc tumors where AEG-1 was detected almost exclusively in the cytoplasm, a feature observed for overexpressed AEG-1 in tumors (2). Alb/AEG-1/c-Myc tumors showed a further increase in cytoplasmic AEG-1 staining (Fig. 1D, top row). Low level nuclear c-Myc was detected in WT and Alb/AEG-1 liver while c-Myc overexpression was detected both in the nucleus and cytoplasm in Alb/c-Myc and Alb/AEG-1/c-Myc tumors (Fig. 1D, 2nd row). The tumors were positive for AFP (Fig. 1D, 3rd row). Compared to WT liver, increased PCNA staining was detected both in Alb/AEG-1 liver and Alb/c-Myc tumor, the intensity of the staining being more pronounced in Alb/c-Myc tumors (Fig. 1D, bottom row). The intensity of PCNA staining was markedly augmented in Alb/AEG-1/c-Myc mice (Fig. 1D, bottom row). PCNA positive cells per field for WT, Alb/AEG-1, Alb/c-Myc and Alb/AEG-1/c-Myc were 0.75 ± 0.35, 12 ± 4, 14 ± 3, and 45 ± 7, respectively, with counts from 9 independent fields. These finding indicate that both AEG-1 and c-Myc are capable of stimulating proliferation, however, their combinatorial effect is significantly more pronounced.

The response of these 4 groups of mice to DEN-induced hepatocarcinogenesis was checked next. We chose the initial time point of 28 weeks, when Alb/AEG-1 mice develop HCC

while WT mice do not (8). Very few isolated nodules, less than 2-mm in size, were detected in WT mice (Table 2 & Fig. 2A). The number of nodules was significantly increased in all three other groups. However, the total number and size of the nodules were significantly increased in Alb/AEG-1/c-Myc mice (Table 2). More importantly, at 33 weeks the whole liver of Alb/AEG-1/c-Myc mice was converted into HCC with lung metastases (Table 2 & Fig. 2A). Probability analysis of these mice demonstrated that although all groups showed very low probability of developing no tumors, the probability of having increased number of tumors was high in Alb/c-Myc mice and was markedly high in Alb/AEG-1/c-Myc mice (Fig. 2B). Similar pattern of probability was observed when size of the tumors was used as variables (Fig. S3 & S4). Histological analysis at 28 wks showed HCC developing on a steatotic background in Alb/AEG-1 mice, Alb/c-Myc mice showed hypercellular HCC while Alb/AEG-1/c-Myc mice presented with a mixed phenotype (Fig. 2C). The metastatic lung nodules stained positively for AFP, AEG-1 and c-Myc confirming their hepatic origin (Fig. 2D & E).

We analyzed primary hepatocytes from these mice to interrogate the contribution of AEG-1 and c-Myc to different hallmarks of cancer. *In vitro*, WT hepatocytes might replicate once before senescing ~72-96 h. In an 8-day assay measuring proliferation by MTT and BrdU incorporation assays, AEG-1 and c-Myc alone provided significant proliferative advantage *versus* WT (Fig. 3A, top and middle panels). However, the proliferative advantage provided by overexpression of both AEG-1 and c-Myc was markedly higher compared to either oncogene alone. Culturing the hepatocytes in basal medium containing no growth factor (insulin) extended these observations. In this scenario, overexpression of AEG-1 in Alb/AEG-1 or Alb/AEG-1/c-Myc group showed equal level of protection which was markedly higher than that of WT, while overexpression of c-Myc alone provided small albeit significant protection, indicating that it is AEG-1 that contributes to growth factor-independent survival (Fig. 3A, bottom panel). To obtain insights into which pro-survival pathways provide survival advantage we analyzed the activation profile of oncogenic signal transduction pathways on day 1 and day 7 of culture. Sustained activation of signaling pathways at day 7 indicates that these pathways might contribute to survival and proliferative advantages in long-term culture, and hence *in vivo*. It should be noted that the Western blots for day 1 and day 7 were performed separately so that comparison was analyzed among the four groups in each time point rather than between day 1 and day 7. EGFR activation was observed upon overexpression of either AEG-1 or c-Myc, and this activation was further augmented in Alb/AEG-1/c-Myc, which was sustained up to day 7 (Fig. 3B). Similar findings were observed for EGFR downstream signaling molecules, AKT, ERK1/2 and p38 MAPK, and for STAT3, c-Met and c-Src (Fig. 3B). Robust upregulation of p38 MAPK was observed on day 7 only in Alb/AEG-1/c-Myc mice. Upregulation of anti-apoptotic molecules, Bcl-2, Xiap and Survivin, but not Bcl-x_L and Ciap1, was observed with either oncogene alone which was further augmented in Alb/AEG-1/c-Myc mice and sustained until day 7 (Fig. 3C).

We previously demonstrated that overexpression of AEG-1 protects hepatocytes from senescence (8). Analysis of senescence by γ-H2AX foci assay demonstrated profound induction of senescence in WT hepatocytes by day 7 of culture (Fig. 4). Very few isolated γ-

H2AX foci were detected in Alb/AEG-1 and Alb/AEG-1/c-Myc hepatocytes while a few foci were observed in Alb/c-Myc hepatocytes. These findings were also confirmed by senescence-associated β-galactosidase assay (Fig. S5). These findings reflect c-Myc-induced senescence as described before (28) which might be overcome by overexpression of AEG-1. Collectively, activation of pro-survival and proliferative pathways, upregulation of anti-apoptotic proteins and inhibition of senescence contribute to the aggressive behavior observed in Alb/AEG-1/c-Myc mice.

We next analyzed transformation by focus formation assay using primary hepatocytes. c-Myc expression alone provided a greater transforming advantage over AEG-1, however, the combination of the two oncogenes augmented transformation further (Fig. 5A). As a corollary we performed colony formation assays for three weeks in which the hepatocytes were plated on an endogenous matrix which was created by first plating 804G cells that were then gently treated with alkaline solution to remove the cells leaving behind the matrix proteins. WT hepatocytes formed no colonies while Alb/AEG-1 and Alb/c-Myc hepatocytes formed small colonies. However, the colonies formed by Alb/AEG-1/c-Myc hepatocytes were markedly increased in number as well as in size (Fig. 5B). In Matrigel invasion assays, c-Myc overexpression conferred more invasive advantage over AEG-1, and together AEG-1 and c-Myc increased invasion further (Fig. 5C). To obtain insights into the molecular mechanism of these phenomena we checked expression profiles of key players regulating epithelial-mesenchymal transition (EMT) (Fig. 5D). The changes in EMT regulators and markers were more pronounced on day 7 of culture. E-cadherin level was decreased only in Alb/c-Myc mice but not in other 3 groups (Fig. 5D). It was documented previously that E-cadherin is downregulated in the livers of only c-Myc transgenic mouse but not in c-Myc/TGFα or c-Myc/E2F1 double transgenic mice (29). Increased N-cadherin levels were observed only in Alb/AEG-1/c-Myc on day 7. A decrease in ZO1 and Claudin-1, and increases in TCF8, Snail, Slug, Vimentin and SPARC were observed in the transgenics when compared to WT mice. Vimentin and SPARC expression could not be detected on day 1 of culture. A robust increase in the EMT-inducing transcription factors Snail and Slug was observed only in Alb/AEG-1/c-Myc at day 7. Additionally, activation of β-catenin, and TGFβ and its downstream signaling, indicated by activation of Smad-2 and Smad-3, was observed for Alb/AEG-1/c-Myc, especially at day 7. These findings suggest that Alb/AEG-1/c-Myc maintains a sustained EMT phenotype that might contribute to invasion and metastasis.

To obtain insights into the molecular mechanism by which AEG-1 and c-Myc cooperate to promote the aggressive hepatocarcinogenic phenotype we performed RNA-Seq analysis using liver samples from naïve adult WT, Alb/AEG-1, Alb/c-Myc and Alb/AEG-1/c-Myc mice. With an absolute fold-change of >2-fold, 30 and 35 genes showed differential change in Alb/AEG-1 and Alb/c-Myc, respectively, *versus* WT. However, a staggering number of 258 genes showed differential change in Alb/AEG-1/c-Myc vs WT (Fig. 6A and Table S1). Out of these 258 genes, 121 showed upregulation and 137 showed downregulation (Table S1). While some genes showed common changes in single and double transgenics, when compared to WT, Alb/AEG-1/c-Myc mice showed exclusive and robust change in expression of 71 genes (Fig. S6A). We performed biological processes and pathway analysis

using the software DAVID. Among the biological processes differentially regulated in Alb/AEG-1/c-Myc mice two major classes were prominent, (i) cell cycle and cell division, and (ii) metabolic processes including lipid metabolic processes (Table S2). Pathway analysis showed a differential change in MAPK signaling pathways, metabolic signaling and complement and coagulation cascade pathways in Alb/AEG-1/c-Myc *versus* WT (Table S3). We also performed network analysis using Ingenuity software. The top three networks of genes that showed significant changes in Alb/AEG-1/c-Myc *versus* WT include (i) cancer, cellular function and maintenance; (ii) lipid metabolism and (iii) cell death and survival (Fig. S6B). These networks and pathway analyses included gene ontology that is already well-known and genes regulated by c-Myc and AEG-1 as described in previous studies (8, 24, 30, 31). Additionally changes in many of these genes in Alb/AEG-1/c-Myc liver have also been observed in human HCC (a review of the literature is provided in Table S4). Very interestingly we observed robust upregulation of several non-coding RNAs, Rian, Mirg and Meg3, only in Alb/AEG-1/c-Myc group (Table S1). The overexpression of these three non-coding RNAs was confirmed by RT-PCR (Fig. 6B & Fig. S7A). We next attempted to knockdown these 3 ncRNAs by 4 different siRNAs for Rian and Meg3 and 3 different siRNAs for Mirg (Table S5). For Rian and Mirg 2 independent siRNAs effectively knocked down the corresponding RNA by >50% (Fig. S7B). However, none of the 4 siRNAs worked for Meg3. Knocking down Rian and Mirg significantly inhibited proliferation of Alb/AEG-1/c-Myc hepatocytes and the combination of these two siRNAs inhibited proliferation further (Fig. 6C, left and middle panels). Rian and Mirg siRNA inhibited invasion by Alb/AEG-1/c-Myc hepatocytes (Fig. 6C, right panel). However, the combination did not inhibit invasion further suggesting that these two ncRNAs might regulate same molecules mediating invasion. Knocking down Rian or Mirg resulted in substantial decrease in proliferation markers survivin and PCNA, inhibition of activation of p38 MAPK and downregulation of EMT markers Vimentin and TCF8 (Fig. 6D). There was a small decrease in Snail but no decrease in Slug was observed. These findings suggest that these ncRNAs, induced by AEG-1 and c-Myc, contribute both to proliferative and invasive advantages.

Discussion

We document that overexpression of AEG-1 and c-Myc resulted in spontaneous HCC with lung metastases which takes more than 12 months to develop. Cancer genome sequencing indicates that most cancers require at least five genetic changes to evolve (32). Thus, overexpression of two oncogenes might not be enough for generation of early aggressive disease. Initiation of additional mutations by DEN treatment, therefore, significantly accelerated the aggressive behavior conferred by AEG-1 and c-Myc. RNA-Seq analysis identified unique changes in gene expression only when AEG-1 and c-Myc were overexpressed. The predominant biological processes that were modulated in Alb/AEG-1/c-Myc liver *versus* WT liver involve cell cycle and cell division and metabolic pathways including lipid metabolism. These findings are expected considering the pivotal role of c-Myc in regulating cell cycle and cell division and cellular metabolic processes (24, 33-35). Alb/AEG-1 mice develop steatosis and in this context alteration in lipid metabolism associated genes is also expected (8). Pathways analysis identified changes in the MAPK signaling pathway, which has been documented for AEG-1, metabolic pathways and

complement and coagulation cascade pathways. Indeed, our previous study aimed at characterizing Alb/AEG-1 mouse unraveled a key role of coagulation factors in mediating AEG-1-induced angiogenesis (8). Therefore, the gene expression changes that were observed in Alb/AEG-1/c-Myc mice reflected gene expression changes of either oncogene alone. It should be noted that we used a stringent gene-expression change of >2-fold which limited the genes changed in either Alb/AEG-1 or Alb/c-Myc to a small number. In Alb/AEG-1/c-Myc mice these changes became more pronounced thereby significantly increasing the total number of genes with detectable alterations. These observations suggest that AEG-1 and c-Myc might cooperate to amplify expression of genes regulated by either oncogene alone. This cooperation might be conferred by reciprocal positive regulatory changes, e.g., AEG-1 induces c-Myc by activating Wnt/β-catenin pathway and also by squelching away a c-Myc-specific transcriptional repressor PLZF (2, 19). On the other hand c-Myc itself transcriptionally regulates AEG-1. Whether AEG-1 facilitates transcriptional activity of c-Myc remains to be determined. Although AEG-1 does not bind to DNA, it interacts with p65 subunit of NF-κB and CBP, thereby functioning as a bridging factor between NF-κB and basal transcriptional machinery promoting transcriptional activity of NF-κB (36). Whether a similar relationship exists between AEG-1 and c-Myc needs to be explored.

However, one very striking observation is the induction of ncRNAs as a consequence of overexpression of both AEG-1 and c-Myc. The DLK1-DIO3 genomic region, located on mouse chromosome 12 and on human chromosome 14, codes for genes that are expressed either maternally or paternally (37-40). Rian, Meg3 and Mirg are maternally expressed genes that generate ncRNAs (38). Within these ncRNAs lie several snoRNAs and miRNAs which have been recognized to regulate tumorigenesis in diverse organs (41). Targeted overexpression of Rian and Mirg resulted in spontaneous HCC development in mice (42). The miRNA cluster generated from DLK1-DIO3 region has been implicated to confer a stem-like subtype in human HCC associated with poor survival (43, 44). The overexpression of these ncRNAs in Alb/AEG-1/c-Myc might mediate an aggressive oncogenic phenotype in these mice which is supported by the *in vitro* analysis of proliferation and invasion upon knockdown to these ncRNAs. It is intriguing to observe that overexpression of both AEG-1 and c-Myc is required for expression of these imprinted genes.

In vitro analysis demonstrated that although overexpression of both AEG-1 and c-Myc provided proliferative advantage to hepatocytes, it is AEG-1 that enabled the cells to survive in a harsh environment such as growth factor deprivation. On the contrary, AEG-1 alone did not confer transforming ability to the hepatocytes but contributed to transformation induced by c-Myc overexpression. These findings suggest that c-Myc overexpression is able to transform the cells while AEG-1 overexpression allows these transformed cells to progress further with increasing invasive and metastatic abilities. Compared to Alb/AEG-1 and Alb/c-Myc, Alb/AEG-1/c-Myc showed robust and sustained activation of all pro-survival signaling pathways and multiple EMT modulators. Most importantly, EGF, TGFβ and β-catenin signaling pathways, which are key determinants of all hallmarks of aggressive HCC (45), showed sustained activation in Alb/AEG-1/c-Myc mice. Thus, a combination of gene

expression changes and activation of multiple oncogenic signal transduction pathways contribute to the aggressive behavior conferred by AEG-1 and c-Myc.

In summary, we have generated a novel mouse model of aggressive HCC. Alb/AEG-1/c-Myc mice provide a valuable animal model to inhibit tumor suppressor proteins to analyze consequences of oncogene activation and tumor suppressor mutations during hepatocarcinogenesis. Additionally, this mouse model might be effectively used for monitoring efficacy of novel, targeted therapies.

Supplementary Material

Refer to Web version on PubMed Central for supplementary material.

Acknowledgments

Financial support The present study was supported in part by grants from the James S. McDonnell Foundation and National Cancer Institute Grant R01 CA138540 (DS) and R01 CA134721 (PBF). The VCU Massey Cancer Center Transgenic/Knockout Mouse Facility supported, in part, with funding from NIH-NCI Cancer Center Support Grant P30 CA 016059 provided services in support of this project. PBF holds the Thelma Newmeyer Corman Chair in Cancer Research. DS is the Harrison Endowed Scholar in Cancer Research and a Blick scholar.

Abbreviations

AEG-1	Astrocyte elevated gene-1
EGF	Epidermal growth factor
EGFR	Epidermal growth factor receptor
ERK	Extracellular signal-regulated kinase
MAPK	Mitogen activated protein kinase
STAT3	Signal transducer and activator of transcription 3
PCNA	Proliferating cell nuclear antigen
AFP	α-feto protein
MTT	3-(4,5-Dimethylthiazol-2-Yl)-2,5-Diphenyltetrazolium Bromide

References

1. Sarkar D, Fisher PB. AEG-1/MTDH/LYRIC: Clinical Significance. Adv Cancer Res. 2013; 120:39–74. [PubMed: 23889987]
2. Yoo BK, Emdad L, Su ZZ, Villanueva A, Chiang DY, Mukhopadhyay ND, Mills AS, et al. Astrocyte elevated gene-1 regulates hepatocellular carcinoma development and progression. J Clin Invest. 2009; 119:465–477. [PubMed: 19221438]
3. Zhu K, Dai Z, Pan Q, Wang Z, Yang GH, Yu L, Ding ZB, et al. Metadherin Promotes Hepatocellular Carcinoma Metastasis through Induction of Epithelial-Mesenchymal Transition. Clin Cancer Res. 2011; 17:7294–7302. [PubMed: 21976539]
4. Gong Z, Liu W, You N, Wang T, Wang X, Lu P, Zhao G, et al. Prognostic significance of metadherin overexpression in hepatitis B virus-related hepatocellular carcinoma. Oncol Rep. 2012; 27:2073–2079. [PubMed: 22470125]

5. Yoo BK, Chen D, Su Z-Z, Gredler R, Yoo J, Shah K, Fisher PB, et al. Molecular mechanism of chemoresistance by Astrocyte Elevated Gene-1 (AEG-1). Cancer Res. 2010; 70:3249–3258. [PubMed: 20388796]
6. Yoo BK, Gredler R, Vozhilla N, Su ZZ, Chen D, Forcier T, Shah K, et al. Identification of genes conferring resistance to 5-fluorouracil. Proc Natl Acad Sci U S A. 2009; 106:12938–12943. [PubMed: 19622726]
7. Yoo BK, Santhekadur PK, Gredler R, Chen D, Emdad L, Bhutia SK, Pannell L, et al. Increased RNA-induced silencing complex (RISC) activity contributes to hepatocelllular carcinoma. Hepatology. 2011; 53:1538–1548. [PubMed: 21520169]
8. Srivastava J, Siddiq A, Emdad L, Santhekadur P, Chen D, Gredler R, Shen X-N, et al. Astrocyte elevated gene-1 (AEG-1) promotes hepatocarcinogenesis: novel insights from a mouse model. Hepatology. 2012; 56:1782–1791. [PubMed: 22689379]
9. He XX, Chang Y, Meng FY, Wang MY, Xie QH, Tang F, Li PY, et al. MicroRNA-375 targets AEG-1 in hepatocellular carcinoma and suppresses liver cancer cell growth in vitro and in vivo. Oncogene. 2012; 31:3357–3369. [PubMed: 22056881]
10. Thirkettle HJ, Girling J, Warren AY, Mills IG, Sahadevan K, Leung H, Hamdy F, et al. LYRIC/AEG-1 is targeted to different subcellular compartments by ubiquitinylation and intrinsic nuclear localization signals. Clin Cancer Res. 2009; 15:3003–3013. [PubMed: 19383828]
11. Hui AB, Bruce JP, Alajez NM, Shi W, Yue S, Perez-Ordonez B, Xu W, et al. Significance of dysregulated metadherin and microRNA-375 in head and neck cancer. Clin Cancer Res. 2011; 17:7539–7550. [PubMed: 22031094]
12. Yang Y, Wu J, Guan H, Cai J, Fang L, Li J, Li M. MiR-136 promotes apoptosis of glioma cells by targeting AEG-1 and Bcl-2. FEBS Lett. 2012; 586:3608–3612. [PubMed: 22967897]
13. Zhang B, Liu XX, He JR, Zhou CX, Guo M, He M, Li MF, et al. Pathologically decreased miR-26a antagonizes apoptosis and facilitates carcinogenesis by targeting MTDH and EZH2 in breast cancer. Carcinogenesis. 2011; 32:2–9. [PubMed: 20952513]
14. Kochanek DM, Wells DG. CPEB1 Regulates the Expression of MTDH/AEG-1 and Glioblastoma Cell Migration. Mol Cancer Res. 2013; 11:149–160. [PubMed: 23360795]
15. Lee SG, Su ZZ, Emdad L, Sarkar D, Fisher PB. Astrocyte elevated gene-1 (AEG-1) is a target gene of oncogenic Ha-ras requiring phosphatidylinositol 3-kinase and c-Myc. Proc Natl Acad Sci U S A. 2006; 103:17390–17395. [PubMed: 17088530]
16. Chan KL, Guan XY, Ng IO. High-throughput tissue microarray analysis of c-myc activation in chronic liver diseases and hepatocellular carcinoma. Hum Pathol. 2004; 35:1324–1331. [PubMed: 15668888]
17. Wang Y, Wu MC, Sham JS, Zhang W, Wu WQ, Guan XY. Prognostic significance of cmyc and AIB1 amplification in hepatocellular carcinoma. A broad survey using high-throughput tissue microarray. Cancer. 2002; 95:2346–2352. [PubMed: 12436441]
18. Rao UN, Gollin SM, Beaves S, Cieply K, Nalesnik M, Michalopoulos GK. Comparative genomic hybridization of hepatocellular carcinoma: correlation with fluorescence in situ hybridization in paraffin-embedded tissue. Mol Diagn. 2001; 6:27–37. [PubMed: 11257209]
19. Thirkettle HJ, Mills IG, Whitaker HC, Neal DE. Nuclear LYRIC/AEG-1 interacts with PLZF and relieves PLZF-mediated repression. Oncogene. 2009; 28:3663–3670. [PubMed: 19648967]
20. Sandgren EP, Quaife CJ, Pinkert CA, Palmiter RD, Brinster RL. Oncogene-induced liver neoplasia in transgenic mice. Oncogene. 1989; 4:715–724. [PubMed: 2543942]
21. Wu Y, Renard CA, Apiou F, Huerre M, Tiollais P, Dutrillaux B, Buendia MA. Recurrent allelic deletions at mouse chromosomes 4 and 14 in Myc-induced liver tumors. Oncogene. 2002; 21:1518–1526. [PubMed: 11896580]
22. Murakami H, Sanderson ND, Nagy P, Marino PA, Merlino G, Thorgeirsson SS. Transgenic mouse model for synergistic effects of nuclear oncogenes and growth factors in tumorigenesis: interaction of c-myc and transforming growth factor alpha in hepatic oncogenesis. Cancer Res. 1993; 53:1719–1723. [PubMed: 8467484]
23. Simile MM, De Miglio MR, Muroni MR, Frau M, Asara G, Serra S, Muntoni MD, et al. Down-regulation of c-myc and Cyclin D1 genes by antisense oligodeoxy nucleotides inhibits the

expression of E2F1 and in vitro growth of HepG2 and Morris 5123 liver cancer cells. Carcinogenesis. 2004; 25:333–341. [PubMed: 14604889]

24. Coulouarn C, Gomez-Quiroz LE, Lee JS, Kaposi-Novak P, Conner EA, Goldina TA, Onishchenko GE, et al. Oncogene-specific gene expression signatures at preneoplastic stage in mice define distinct mechanisms of hepatocarcinogenesis. Hepatology. 2006; 44:1003–1011. [PubMed: 17006931]
25. Shachaf CM, Kopelman AM, Arvanitis C, Karlsson A, Beer S, Mandl S, Bachmann MH, et al. MYC inactivation uncovers pluripotent differentiation and tumour dormancy in hepatocellular cancer. Nature. 2004; 431:1112–1117. [PubMed: 15475948]
26. Langhofer M, Hopkinson SB, Jones JC. The matrix secreted by 804G cells contains laminin-related components that participate in hemidesmosome assembly in vitro. J Cell Sci. 1993; 105:753–764. [PubMed: 8408302]
27. Anders S, Huber W. Differential expression analysis for sequence count data. Genome Biol. 2010; 11:R106. [PubMed: 20979621]
28. Campaner S, Doni M, Hydbring P, Verrecchia A, Bianchi L, Sardella D, Schleker T, et al. Cdk2 suppresses cellular senescence induced by the c-myc oncogene. Nat Cell Biol. 2010; 12:54–59. [PubMed: 20010815]
29. Calvisi DF, Ladu S, Conner EA, Factor VM, Thorgeirsson SS. Disregulation of E-cadherin in transgenic mouse models of liver cancer. Lab Invest. 2004; 84:1137–1147. [PubMed: 15220935]
30. Lee JS, Chu IS, Mikaelyan A, Calvisi DF, Heo J, Reddy JK, Thorgeirsson SS. Application of comparative functional genomics to identify best-fit mouse models to study human cancer. Nat Genet. 2004; 36:1306–1311. [PubMed: 15565109]
31. Yamashita T, Ji J, Budhu A, Forgues M, Yang W, Wang HY, Jia H, et al. EpCAM-positive hepatocellular carcinoma cells are tumor-initiating cells with stem/progenitor cell features. Gastroenterology. 2009; 136:1012–1024. [PubMed: 19150350]
32. Wood LD, Parsons DW, Jones S, Lin J, Sjoblom T, Leary RJ, Shen D, et al. The genomic landscapes of human breast and colorectal cancers. Science. 2007; 318:1108–1113. [PubMed: 17932254]
33. Cairns RA, Harris IS, Mak TW. Regulation of cancer cell metabolism. Nat Rev Cancer. 2011; 11:85–95. [PubMed: 21258394]
34. Grandori C, Cowley SM, James LP, Eisenman RN. The Myc/Max/Mad network and the transcriptional control of cell behavior. Annu Rev Cell Dev Biol. 2000; 16:653–699. [PubMed: 11031250]
35. Dang CV. c-Myc target genes involved in cell growth, apoptosis, and metabolism. Mol Cell Biol. 1999; 19:1–11. [PubMed: 9858526]
36. Sarkar D, Park ES, Emdad L, Lee SG, Su ZZ, Fisher PB. Molecular basis of nuclear factor-kappaB activation by astrocyte elevated gene-1. Cancer Res. 2008; 68:1478–1484. [PubMed: 18316612]
37. Schmidt JV, Matteson PG, Jones BK, Guan XJ, Tilghman SM. The Dlk1 and Gtl2 genes are linked and reciprocally imprinted. Genes Dev. 2000; 14:1997–2002. [PubMed: 10950864]
38. Irving MD, Buiting K, Kanber D, Donaghue C, Schulz R, Offiah A, Mohammed SN, et al. Segmental paternal uniparental disomy (patUPD) of 14q32 with abnormal methylation elicits the characteristic features of complete patUPD14. Am J Med Genet A. 2010; 152A:1942–1950. [PubMed: 20602488]
39. Benetatos L, Hatzimichael E, Londin E, Vartholomatos G, Loher P, Rigoutsos I, Briasoulis E. The microRNAs within the DLK1-DIO3 genomic region: involvement in disease pathogenesis. Cell Mol Life Sci. 2013; 70:795–814. [PubMed: 22825660]
40. Stadtfeld M, Apostolou E, Akutsu H, Fukuda A, Follett P, Natesan S, Kono T, et al. Aberrant silencing of imprinted genes on chromosome 12qF1 in mouse induced pluripotent stem cells. Nature. 2010; 465:175–181. [PubMed: 20418860]
41. Seitz H, Royo H, Bortolin ML, Lin SP, Ferguson-Smith AC, Cavaille J. A large imprinted microRNA gene cluster at the mouse Dlk1-Gtl2 domain. Genome Res. 2004; 14:1741–1748. [PubMed: 15310658]

42. Wang PR, Xu M, Toffanin S, Li Y, Llovet JM, Russell DW. Induction of hepatocellular carcinoma by in vivo gene targeting. Proc Natl Acad Sci U S A. 2012; 109:11264–11269. [PubMed: 22733778]

43. Toffanin S, Hoshida Y, Lachenmayer A, Villanueva A, Cabellos L, Minguez B, Savic R, et al. MicroRNA-based classification of hepatocellular carcinoma and oncogenic role of miR-517a. Gastroenterology. 2011; 140:1618–1628. e1616. [PubMed: 21324318]

44. Luk JM, Burchard J, Zhang C, Liu AM, Wong KF, Shek FH, Lee NP, et al. DLK1-DIO3 genomic imprinted microRNA cluster at 14q32.2 defines a stemlike subtype of hepatocellular carcinoma associated with poor survival. J Biol Chem. 2011; 286:30706–30713. [PubMed: 21737452]

45. Villanueva A, Newell P, Chiang DY, Friedman SL, Llovet JM. Genomics and signaling pathways in hepatocellular carcinoma. Semin Liver Dis. 2007; 27:55–76. [PubMed: 17295177]

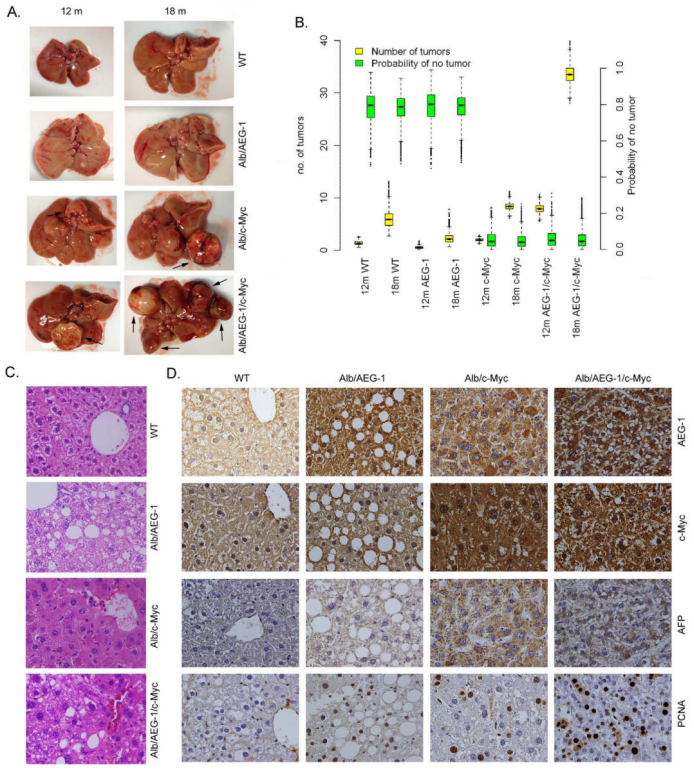

Fig. 1.

AEG-1 and c-Myc overexpression markedly augments spontaneous hepatocarcinogenesis. A. Photograph of livers of the indicated groups at 12 and 18 months. B. Bayesian analysis to determine probabilities of no tumor and number of tumors. C. H & E staining of liver sections at 18 m showing steatosis in Alb/AEG-1, hyperproliferative HCC in Alb/c-Myc and HCC in a mixed background of steatosis and hyperproliferation in Alb/AEG-1/c-Myc. D. Liver sections at 18 m from the indicated groups were stained for AEG-1, c-Myc, AFP and PCNA. The panels show representative photomicrographs. For C & D, magnification 400X.

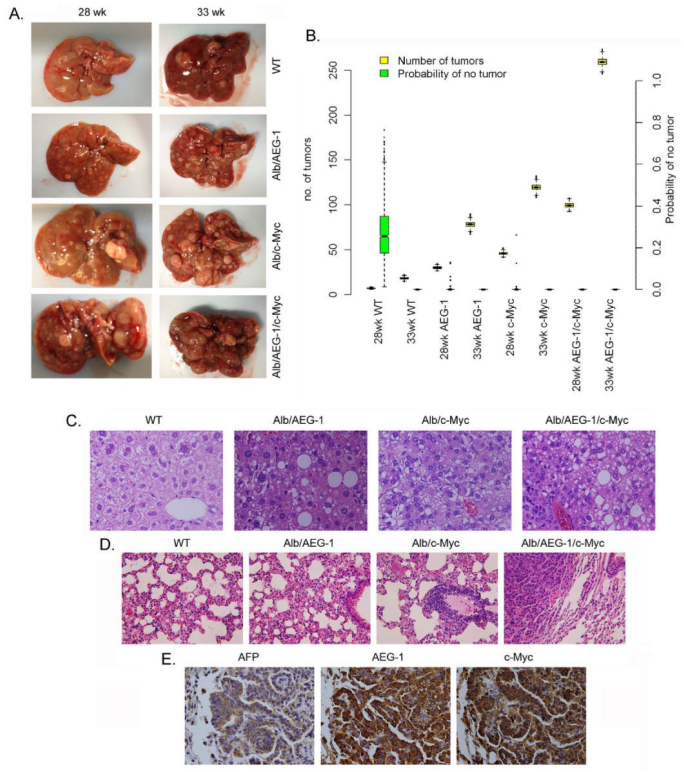

Fig. 2.

DEN-induced HCC and metastases are markedly increased in Alb/AEG-1/c-Myc mice. A. Photograph of livers of the indicated groups at 28 and 33 weeks. B. Bayesian analysis was performed in DEN-treated 28 and 33 weeks old WT, Alb/AEG-1, Alb/c-Myc and Alb/AEG-1/c-Myc samples. C. H & E staining of liver sections at 33 wks. D. H & E staining of lung sections at 33 wks. Asterisk indicates metastatic tumors. E. Lung tumors were stained for AFP, AEG-1 and c-Myc to demonstrate metastases from the liver. For C-E, magnification 400X.

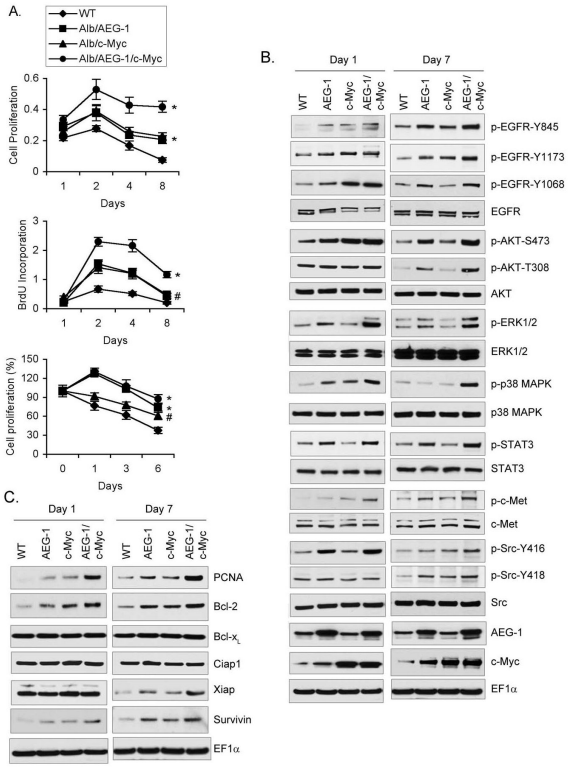

Fig. 3.

Cell proliferation and survival, and pro-survival signaling pathways are activated in Alb/AEG-1/c-Myc hepatocytes. A. Top panel, Cell proliferation in standard media was determined by MTT assay. Middle panel, BrdU incorporation assay. Bottom panel, Cell proliferation in basal media without insulin was determined by MTT assay. Data represent mean ± SEM of 3 independent experiments. *: $p<0.01$ *versus* WT; #: $p<0.05$ *versus* WT. B. Western blot analysis of the indicated proteins in cell survival pathways. C. Western blot analysis of the indicated anti-apoptotic proteins. For B & C, for each blot EF1α was used for loading control and one representative EF1α blot is shown here.

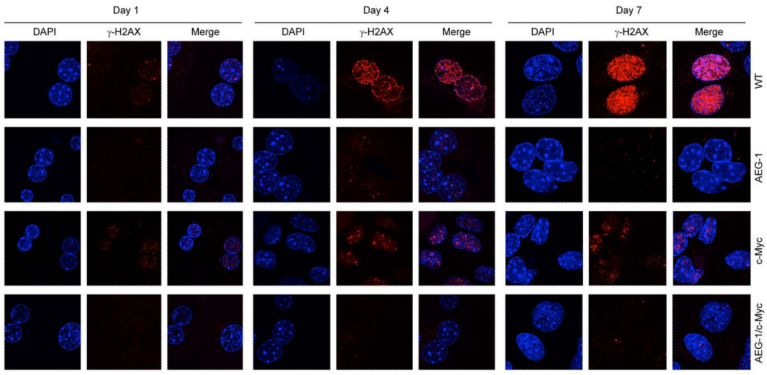

Fig. 4.

Senescence is inhibited in Alb/AEG-1/c-Myc hepatocytes. Hepatocytes from the indicated groups were stained with DAPI for nucleus and for γ-H2AX at day 1, 4 and 7 of culture. The images were analyzed by a confocal laser scanning microscope. Magnification 630X.

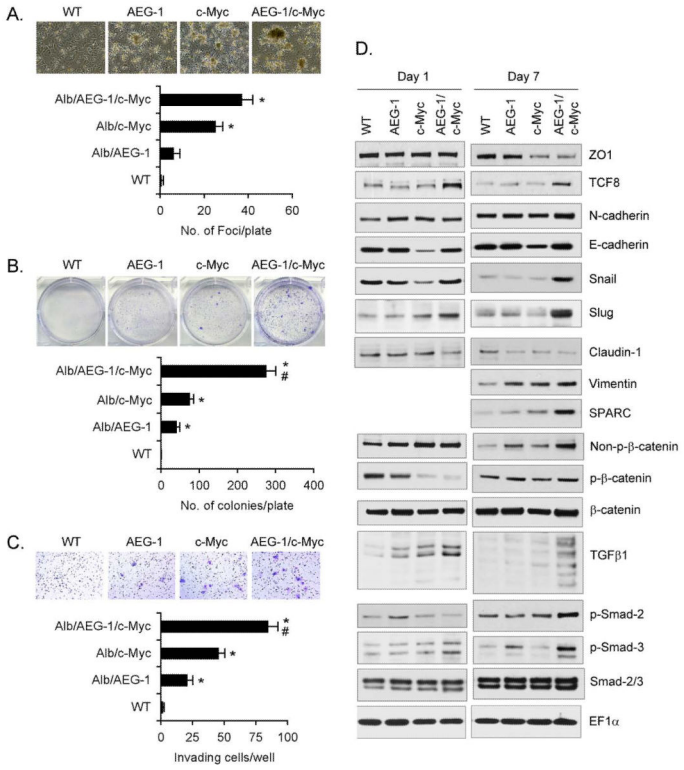

Fig. 5.

Transformation and invasion are augmented in Alb/AEG-1/c-Myc hepatocytes. A. Top panel, photomicrographs of the cells. Bottom panel, graphical representation of quantification of the number of foci. B. Top panel, photographs of the plates showing the colonies. Bottom panel, graphical representation of quantification of the number of colonies. C. Matrigel invasion assay. Top panel, photomicrographs of the invading cells. Bottom panel, graphical representation of the quantification of the number of invading cells. For A-C, data represent mean ± SEM of 3 independent experiments. *: $p<0.01$ vs WT; #: $p<0.05$ vs Alb/AEG-1 or Alb/c-Myc. D. Western blot analysis of the indicated proteins regulating EMT. For each blot EF1α was used for loading control and one representative EF1α blot is shown here.

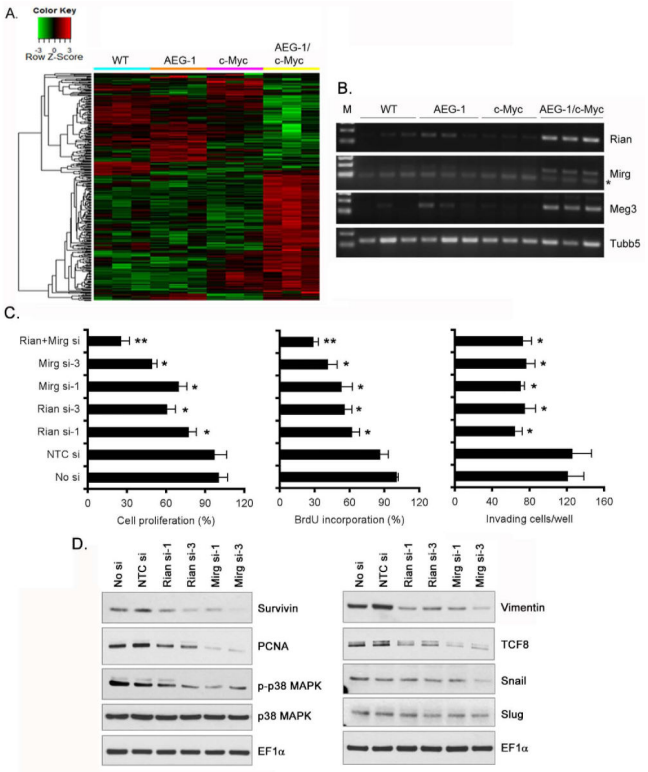

Fig. 6.

AEG-1 and c-Myc overexpression specifically induces ncRNAs. A. Heat map showing differential gene expression in the indicated groups. B. RT-PCR analysis for Rian, Mirg and Meg3 in the indicated groups. Tubb5 was used as a control. Asterisk indicates non-specific band. C. Analysis of cell proliferation and invasion upon knockdown of Rian and Mirg. Left panel, Cell proliferation by MTT assay at 72 h after transfection. Middle panel, BrdU incorporation assay at 72 h after transfection. Right panel, Matrigel invasion assay at 48 h after transfection. Rian and Mirg ncRNAs were knocked down by two individual siRNA either alone or in combination. NTC si: control scrambled siRNA. Data represent mean ± SEM of 3 independent experiments. *: $p<0.05$ vs WT; **: $p<0.01$ vs No si or NTC si. D. Western blot analysis of the indicated proteins. For each blot EF1α was used for loading control and one representative EF1α blot is shown here.

Table 1

No. of liver nodules and lung metastasis score in spontaneously developed HCC.

		12m						18m					
	ID#	**1-2mm**	**2-5mm**	**5-10mm**	**10-20mm**	**>20mm**	**ID#**	**1-2mm**	**2-5mm**	**5-10mm**	**10-20mm**	**>20mm**	**Lung mets**
WT	104						17						
	108						18						
	113	1					28						
	114						29						
	116						33	7					
	125						54						
	127						72						
	130						74						
	134						84						
							86						
							92	6					
							93						
AEG-1	109						9						
	121						25						
	124						26						
	131						27						
	141						46	1					
	142						50	4					
	145	1					58						
	154						73						
	155						76						
	158						78						
							96						
							98	3					
							100						
							107						

		12m						18m					
	ID#	**1-2mm**	**2-5mm**	**5-10mm**	**10-20mm**	**>20mm**	**ID#**	**1-2mm**	**2-5mm**	**5-10mm**	**10-20mm**	**>20mm**	**Lung mets**
							115						
							118						
							119						
							120						
c-Myc	123	1		1			31	1			4		
	138	3					32			3	2	4	
	147	4	1				35		2		1		
	149		2				49			1	1	1	
	150	6					55		6		8		
	151	3	4				59					3	
	152	1	3				75		5		1		
	153	5					77			3			
	156	7					87			1	1		
	159	1	2				97		6		2		
	160	4	5				102		3		7		
	161	3	7				118			1		1	
							126		5	1		1	
							139		4	3	2		
							143			2	3		
							144			5	1		
AEG-1/c-Myc	110		3		1		19			5	9	8	+
	111	5		6			34		1	4	11	7	+
	112	4	4	2			47			7	14	4	+
	122			3			48			8	10	9	+
	129		1		1		61	Whole liver					+
	137					1	62			19	5	6	+
	140				2		65	Whole liver					+
	146			4			68	Whole liver					+

		12m						18m					
	ID#	1-2mm	2-5mm	5-10mm	10-20mm	>20mm	ID#	1-2mm	2-5mm	5-10mm	10-20mm	>20mm	Lung mets
	148			3			94			6	17	12	+
	157				1		95		2	8	5	11	+

Table 2

No. of liver nodules and lung metastasis score in DEN-treated mice.

		28 wks						33 wks					
	ID#	**1-2mm**	**2-5mm**	**5-10mm**	**10-20mm**	**>20mm**	**ID#**	**1-2mm**	**2-5mm**	**5-10mm**	**10-20mm**	**>20mm**	**Lung mets**
WT	C10						C41	18		3			
	C13	2					C58		4	4			
	C16	1					C61	10		1			
	C20	5					C82	4					
	C27	3					C86	34		2			
	C29		2				C90	42	12				
	C30		1				C91	4		1			
	C34	1					C93		40	5			
	C35	2					C96	35		2			
							C102	11		1			
							C104	6					
AEG-1	C12	32		2			C79		44	12	3		
	C22	27					C89		24	19	4	1	
	C50	49			1		C92		30		6	1	
	C51		48	1			C95		82	4	4	1	
	C65	33	12				C97		72	3	1	2	
	C81	49					C106		56	11	5	2	
	C83	55		2			C111		48	4	4	1	
c-Myc	C3	86		5		1	C37		68		5	2	
	C9	45		3	2		C42		119	7	3	1	
	C11	93		5		1	C57		74	5		2	
	C31	59	5			2	C60		67	6	2	2	
	C49	52		4			C98		80	4	1	3	
	C52	32		3	3	1	C100		91	7	3	3	
	C54	41		4			C101		100	8	1	1	
	C63	52		3	1		C103		152	3	4	2	

Hepatology. Author manuscript; available in PMC 2016 March 01.

		28 wks						33 wks					
	ID#	**1-2mm**	**2-5mm**	**5-10mm**	**10-20mm**	**>20mm**	**ID#**	**1-2mm**	**2-5mm**	**5-10mm**	**10-20mm**	**>20mm**	**Lung mets**
	C64	40											
AEG-1/c-Myc	C4		56	3	1	1	C36	Whole liver					+
	C17		123	1	1	1	C69	Whole liver					+
	C21		120		3	4	C75	Whole liver					+
	C28		59		3	2	C78	Whole liver					+
	C45		57		5		C84	Whole liver					+
	C46		60	3		5	C87	Whole liver					+
	C48		43	10	5	3	C88	Whole liver					+
	C55		71	9	2	4	C94	Whole liver					+
	C56		28	12	2	3	C99	Whole liver					+
	C80		84	1	2	4	C105	Whole liver					+
							C107	Whole liver					+
							C109	Whole liver					+
							C110	Whole liver					+